

# Delayed cell cycle pathway modulation facilitates recovery after spinal cord injury

Junfang Wu,<sup>1,\*</sup> Bogdan A. Stoica,<sup>1</sup> Michael Dinizo,<sup>1</sup> Ahdeah Pajoohesh-Ganji,<sup>2</sup> Chunshu Piao<sup>1</sup> and Alan I. Faden<sup>1</sup>

<sup>1</sup>Department of Anesthesiology; and Center for Shock, Trauma and Anesthesiology Research (STAR); University of Maryland School of Medicine; Baltimore, MD USA;

<sup>2</sup>Department of Anatomy and Regenerative Biology; George Washington University Medical School; Washington DC, USA

**Key words:** spinal cord injury, cyclin-dependent kinases, cell cycle pathway, flavopiridol, oligodendrocytes, myelination, astrocytes, inflammation, neuron

**Abbreviations:** CDKIs, cyclin-dependent kinase inhibitors; CDKs, cyclin-activated kinases; pRb, phosphorylated retinoblastoma protein; SCI, spinal cord injury; BBB, basso, beattie and bresnahan locomotor rating scale; CBS, combination behavioral scores

Traumatic spinal cord injury (SCI) causes tissue loss and associated neurological dysfunction through mechanical damage and secondary biochemical and physiological responses. We have previously described the pathobiological role of cell cycle pathways following rat contusion SCI by examining the effects of early intrathecal cell cycle inhibitor treatment initiation or gene knockout on secondary injury. Here, we delineate changes in cell cycle pathway activation following SCI and examine the effects of delayed (24 h) systemic administration of flavopiridol, an inhibitor of major cyclin-dependent kinases (CDKs), on functional recovery and histopathology in a rat SCI contusion model. Immunoblot analysis demonstrated a marked upregulation of cell cycle-related proteins, including pRb, cyclin D1, CDK4, E2F1 and PCNA, at various time points following SCI, along with downregulation of the endogenous CDK inhibitor p27. Treatment with flavopiridol reduced induction of cell cycle proteins and increased p27 expression in the injured spinal cord. Functional recovery was significantly improved after SCI from day 7 through day 28. Treatment significantly reduced lesion volume and the number of Iba-1<sup>+</sup> microglia in the preserved tissue and increased the myelinated area of spared white matter as well as the number of CC1<sup>+</sup> oligodendrocytes. Furthermore, flavopiridol attenuated expression of Iba-1 and glactin-3, associated with microglial activation and astrocytic reactivity by reduction of GFAP, NG2 and CHL1 expression. Our current study supports the role of cell cycle activation in the pathophysiology of SCI and, by using a clinically relevant treatment model, provides further support for the therapeutic potential of cell cycle inhibitors in the treatment of human SCI.

## Introduction

Traumatic spinal cord injury (SCI) causes tissue loss and associated neurological dysfunction due to both mechanical damage and secondary biochemical and physiological responses.<sup>1-6</sup> Mechanisms of secondary injury include a complex cellular response through the activation and/or suppression of a large number of transcriptional pathways in a heterogeneous cell population. These mechanisms include neuronal cell death, loss of oligodendrocytes, inflammation and reactive astrogliosis.<sup>1,7</sup> Effective clinical strategies will likely include either combination of selective inhibitors of secondary injury factors or single drugs that modulate multiple injury components.

Our comprehensive gene profiling analysis of rat spinal cord after contusion injury has demonstrated upregulation of a cluster of cell cycle-related genes, including *c-myc*, *Gadd45*, cyclin D1, proliferating cell nuclear antigen (PCNA), cyclin G, cyclin-dependent kinase 4 (CDK4), E2 promoter binding factor 5 (E2F5) and retinoblastoma protein (Rb) at 4 h and 24 h after SCI.<sup>8</sup> The cascade of molecular events linking activation of cell cycle to

neuronal apoptosis involves formation of the cyclin D1-CDK4/6 complex, activation of CDK4/6, phosphorylation of Rb, dissociation of Rb-E2F complex and activation of E2F transcriptional activity.<sup>9</sup> The latter can contribute to increased transcription of pro-apoptotic molecules such as caspases 3, 9 and 8 and Apaf-1 or pro-apoptotic Bcl-2 family members.<sup>10,11</sup> Aberrant cell cycle activation not only induces apoptosis of post-mitotic cells (neurons and mature oligodendrocytes), but also initiates proliferation and activation of mitotic cells (microglia/macrophages, astrocytes, precursor cells) in multiple experimental models, including SCI,<sup>8,12-14</sup> brain injury<sup>15-17</sup> and cerebral ischemia.<sup>18,19</sup> Thus, identification of common molecular pathways, including the role of cell cycle proteins involved in both neuronal death and reactive gliosis, may help to clarify the pathobiology of CNS injury and lead to the elucidation of novel therapeutic targets.

CDK inhibitors have been widely studied as cancer therapeutics due to their potential role in restoring control of the cell cycle.<sup>20</sup> Flavopiridol is a potent competitive CDK inhibitor, acting on all CDKs. We have reported previously in reference 13 that flavopiridol, when administered centrally by intrathecal

\*Correspondence to: Junfang Wu; Email: [jwu@anes.umm.edu](mailto:jwu@anes.umm.edu)  
Submitted: 02/18/12; Revised: 03/24/12; Accepted: 03/26/12  
<http://dx.doi.org/10.4161/cc.20153>

injection 30 min post-injury and continuing for 7 d, significantly improves motor recovery and reduces lesion volume at 28 d.

In the present study, we examined the effects of injury on cell cycle expression and whether the delayed systemic administration of flavopiridol can promote recovery after SCI. Delayed treatment is a more clinically relevant paradigm and may provide additional advantages to current clinical options, as methylprednisolone has not proven effective when administered more than 8 h after injury.<sup>21</sup> To test this hypothesis we investigated the effects of systemic flavopiridol administration, beginning 24 h post-injury.

## Results

**Cell cycle activation is induced after SCI and attenuated by systemic administration of flavopiridol.** To evaluate the effect of SCI on cell cycle activation, we first systematically examined cell cycle pathway changes from 1 to 28 d after contusion injury. Quantitative analysis of western blots showed that Rb was rapidly phosphorylated by day 1 and subsequently declined after 3 d post-lesion. The expression of cyclin D1 and CDK4 was highly upregulated, beginning at day 1 (2- to 1.5-fold) and remaining elevated for at least 4 weeks after SCI (Fig. 1B). E2F1 expression levels were rapidly increased by day 1, declined by 3 d and remained 1.5–2.8-fold that of controls from 1–4 weeks post-injury. Levels of PCNA protein in spinal cord tissue was approximately 4–5-fold that of controls by 3 d post-injury (Fig. 1B). In contrast, the endogenous CDK inhibitor p27 was robustly downregulated to 10% of control levels at 1–3 d post-injury and remained at 30–40% of control values during 1–4 weeks (Fig. 1).

Western blot analysis demonstrated that flavopiridol treatment significantly reduced the SCI-induced increase in Rb phosphorylation (ser780, Fig. 2A and B) and expression of cyclin D1 (Fig. 2C and D) at 3 d post-injury. Expression levels of CDK4 were also markedly attenuated by flavopiridol at 4 weeks after SCI (Fig. 2E and F). In contrast, inhibition of p27 after SCI was reversed by flavopiridol treatment beginning at 7 d (data not shown) and significantly at 4 weeks post-injury (Fig. 2G–H).

**Delayed systemic treatment with flavopiridol improves recovery of locomotor function and reduces secondary tissue damage.** At day 1 after SCI, all rats had a BBB score of 0 or 1, indicating nearly complete loss of motor function. Between 1 and 4 weeks, flavopiridol-treated rats showed improved neurological function compared with vehicle treatment as indicated by BBB scores (Fig. 3A). By day 7 after injury, flavopiridol-treated rats had significantly improved BBB scores ( $7.41 \pm 0.61$ ,  $n = 11$ ) compared with vehicle-treated animals ( $4.88 \pm 0.34$ ,  $n = 13$ ). Significant differences between groups remained through 28 d after injury ( $11.09 \pm 0.60$  for flavopiridol vs.  $8.5 \pm 0.32$  for vehicle,  $p < 0.05$  with two-way ANOVA followed by repeated-measures). Moreover, 82% of the flavopiridol-treated rats had achieved a score of 8 or higher by 14 d, as compared with only 23% in the vehicle-treated group.

In addition to the BBB score, neurological functional deficits were estimated using a battery of behavioral tests (the combined behavioral score, CBS) for evaluation of overall hind limb

sensory-motor deficits.<sup>22</sup> By day 1, rats with nearly complete injury had a score of 100. By day 7 after injury, animals in the vehicle group had reached  $82.9\% \pm 1.8$ , while flavopiridol treatment resulted in a significantly greater reduction to  $63.3\% \pm 3.8$  (Fig. 3B). This improvement remained through 28 d after injury ( $44.8\% \pm 3.4$  for flavopiridol vs.  $62.3 \pm 1.9$  for vehicle,  $p < 0.05$  with two-way ANOVA followed by repeated-measures).

SCI-induced lesion volume/cavity formation was measured with GFAP/DAB staining at 4 weeks after SCI and analyzed by unbiased stereological techniques. The average lesion volume assessed for the vehicle group was  $12.98 \pm 0.63 \text{ mm}^3$ , and flavopiridol treatment significantly reduced lesion cavity with an average lesion volume of  $7.21 \pm 0.64 \text{ mm}^3$  (Fig. 3D). This reduction occurred in both white and gray matter, with an overall decrease in cavity formation and tissue loss (Fig. 3C).

**Flavopiridol treatment increases the number of oligodendrocytes and myelinated white matter area at 4 weeks after SCI.** To determine if the observed behavioral improvement may relate to increased remyelination of spared axons, spinal cord sections from injured rats perfused at 28 d were stained with eriochrome cyanine, and WM area was quantified at 1-mm intervals rostral and caudal to the injury epicenter (Fig. 4). Flavopiridol treatment significantly increased WM area at the injury epicenter as well as caudal and rostral to the epicenter (Fig. 4B). Representative eriochrome stained sections at 1 mm caudal to the epicenter of each subject illustrate the differences in myelinated WM area between vehicle- and flavopiridol-treated animals (Fig. 4A).

To assess whether increased myelination of axons in the flavopiridol-treated animals might relate to increased oligodendrocyte number, we quantified total mature oligodendrocyte (CC1<sup>+</sup> cells) using the optical fractionator method of unbiased stereology. SCI caused a 41% loss of mature CC1<sup>+</sup> cells from 5 mm rostral to 5 mm caudal the lesion site at 4 weeks after injury (Fig. 4C). Treatment with flavopiridol attenuated SCI-induced loss of CC1<sup>+</sup> cells in the preserved tissue. Figure 4D shows representative images of CC1/DAB staining located in ventromedial white matter from sham, vehicle- and flavopiridol-treated spinal cord sections. There was no difference in CC1<sup>+</sup> cells between vehicle- and flavopiridol-treated sham groups. There was a positive correlation ( $r^2 = 0.9079$ ) between reduction of CBS scores and increased CC1<sup>+</sup> cells, due to flavopiridol treatment following SCI (Fig. 4E).

We also studied the expression of myelin basic protein (MBP) to assess possible treatment-related alterations in myelination in the injured spinal cord. The 21.5 kDa isomer of MBP was significantly upregulated in the flavopiridol-treated group (Fig. 4F). No apparent differences between the groups were found for the other MBP isomers (18.5, 17.0 and 14.0 kDa, Fig. 4G).

**Flavopiridol reduces post-mitotic cellular apoptosis after SCI.** We have shown that central administration of flavopiridol beginning 30 min after SCI reduces apoptosis, evidenced by qualitative assessment of TUNEL and cleaved-caspase 3 staining.<sup>13</sup> To investigate the effects of systemic delayed treatment of flavopiridol on neuronal and oligodendrocyte cell death after SCI, 5-mm segments of spinal cord tissue representing the injury epicenter were assessed at 3 d post-injury for markers of apoptosis

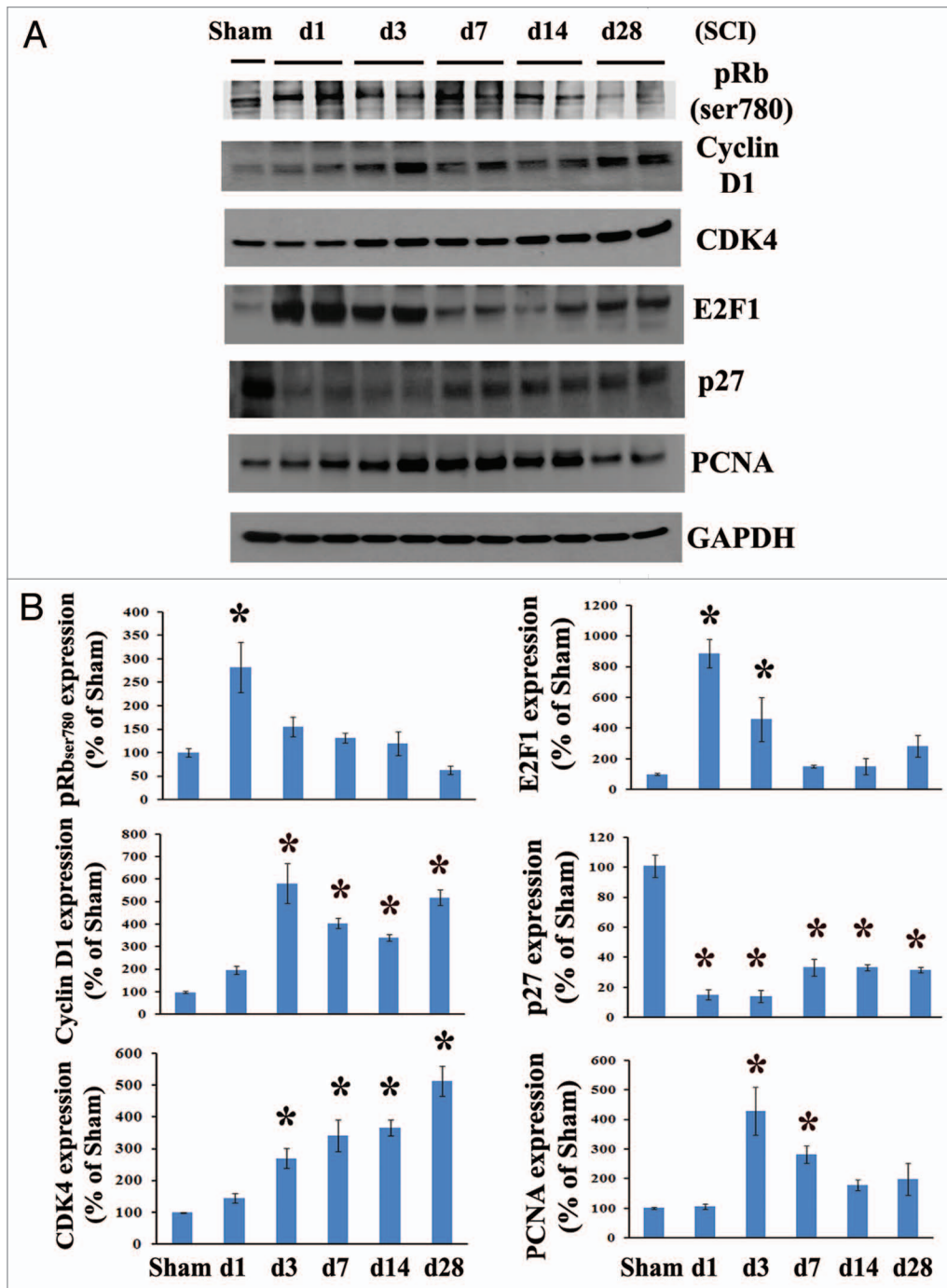


**Figure 1.** Cell cycle activation changes over time following spinal cord contusion in rats. (A) Representative immunoblots for cell cycle-related proteins (pRb, cyclin D1, E2F1, CDK4, PCNA and p27) and the loading control (GAPDH). (B) Expression levels of cell cycle proteins were normalized by GAPDH, as estimated by optical density measurements and expressed as a percentage of sham spinal cord. Quantitative analysis of western blots showed that E2F1 and pRb expression levels were rapidly increased by day 1 and declined after 3 d post lesion. Protein expression of cyclin D1 and CDK4 was highly upregulated starting at 1 d (2- to 1.5-fold) and continuing for at least 4 weeks after SCI. The quantity of PCNA protein in spinal cord tissue was approximately 4-fold that of controls by 3 d and then declined after 1 week post-injury, whereas the endogenous CDK inhibitor p27 was downregulated. \* $p < 0.05$  compared with sham group.  $n = 4$  rats per time point.

by western blots. As shown in **Figure 5A and B**, SCI significantly increased cleavage of fodrin as demonstrated by increased levels of the 150/145 kDa cleavage product of fodrin. Notably, flavopiridol treatment markedly reduced the expression levels of the

cleavage products of fodrin when compared with vehicle-treated samples ( $p < 0.05$ , vs. vehicle).

Neurons, as well as mature oligodendrocytes undergo apoptosis following SCI. We have shown increased oligodendrocyte

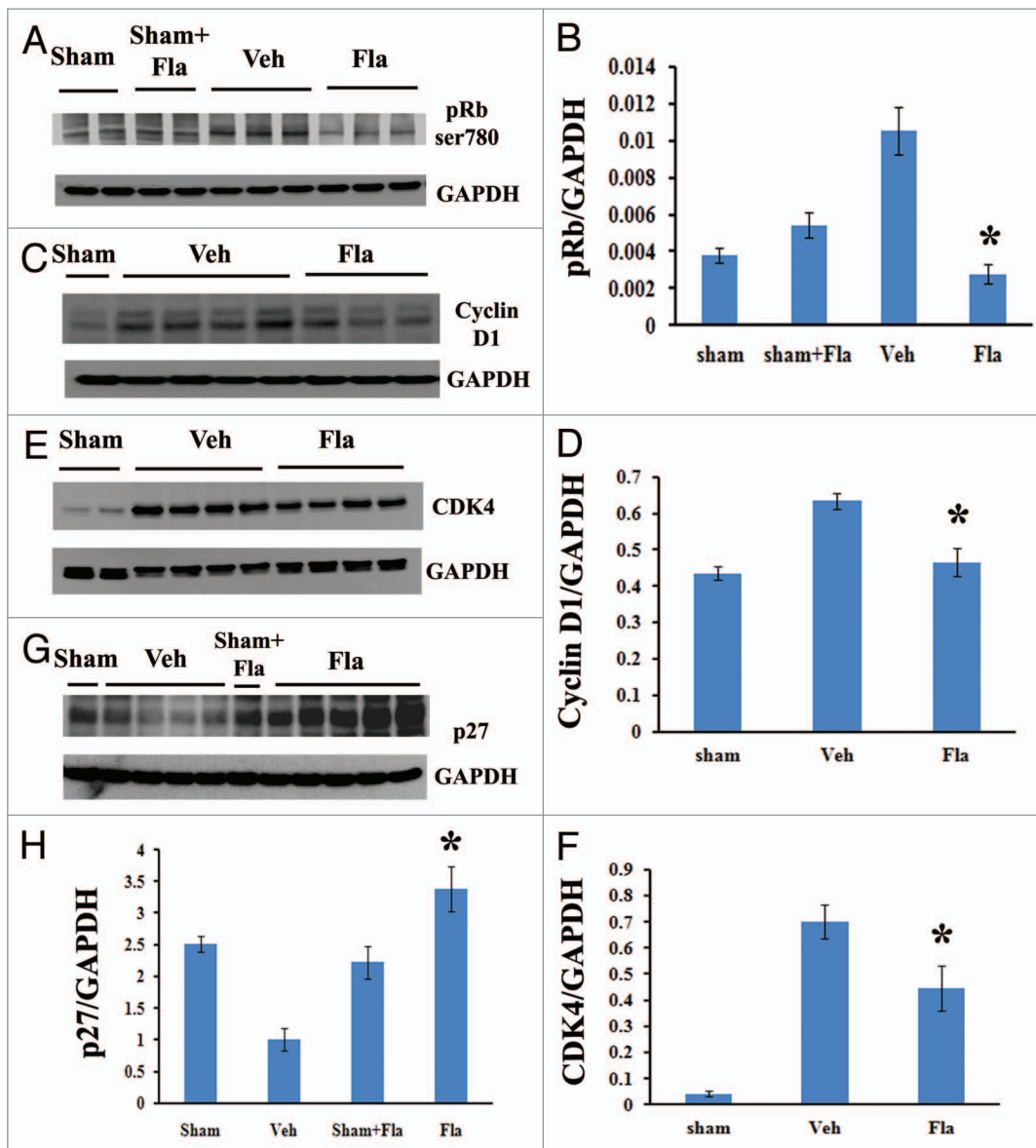


**Figure 2.** Systemic administration of flavopiridol attenuates cell cycle activation after SCI. Western blot analysis showed that flavopiridol treatment significantly reduced the SCI-induced increase in phosphorylation of Rb (ser780, A and B) and expression of cyclin D1 (C and D) at 3 d post-injury. Expression levels of CDK4 were also markedly attenuated by flavopiridol at 4 weeks after SCI (E and F). Inhibition of endogenous CDK inhibitor p27 was significantly rescued by flavopiridol administration at 4 weeks post-injury (G and H). Representative western blots are shown in the left part. Mean values and SEM of protein expression levels normalized to GAPDH are shown in the right part. \* $p < 0.05$  compared with sham group.  $n = 3-5/\text{group}$ .

number following flavopiridol treatment (Fig. 4C). Stereological assessment of surviving neurons was also examined at 4 weeks after SCI (Fig. 5C). SCI resulted in 50% of neuronal cell loss ( $476,506.2 \pm 36,060.4$  vs.  $966,968.5 \pm 23,196.0$  NeuN<sup>+</sup> cells for vehicle and sham samples, respectively), whereas flavopiridol significantly improved neuronal survival at 4 weeks after injury when compared with vehicle-treated samples (Fig. 5C,  $586,324.5 \pm 72,282.2$  vs.  $476,506.2 \pm 36,060.4$  NeuN<sup>+</sup> cells for flavopiridol-treated and vehicle-treated samples, respectively). There was no difference in NeuN<sup>+</sup> cells between sham and flavopiridol-treated sham groups.

**Flavopiridol inhibits astrocyte reactivity and microglial activation.** GFAP is an indicator of astrocyte reactivity associated

with glial scar formation.<sup>23</sup> Western blot analysis showed a significant reduction of GFAP protein expression at 4 weeks post-injury in flavopiridol-treated tissues (Fig. 6A and B,  $p < 0.05$  vs. vehicle treated controls). Immunohistochemistry with GFAP staining (Fig. 6Bf, e and h) confirmed the attenuation of GFAP immunoreactivity with flavopiridol treatment (Fig. 6Bh).

NG2 proteoglycan and the Ig superfamily adhesion molecule the close homolog of L1 (CHL1) are highly expressed by hypertrophic astrocytes at the glial scar, restricting posttraumatic axonal growth.<sup>24-27</sup> As shown by western blot analysis, NG2 glycoprotein and CHL1 levels in spinal cord tissue robustly increased at 4 weeks after our moderate SCI in rats (Fig. 6C). Flavopiridol treatment significantly attenuated the expression of both NG2

glycoprotein and CHL1 ( $p < 0.05$ , vs. vehicle, Fig. 6D and E). We also performed an additional immunohistochemistry study to examine NG2-expressing cell types in our rat SCI contusion model chronically 4 weeks after injury. Immunohistochemistry with NG2 staining (Fig. 6Fa, d and g) confirmed the attenuation of NG2 immunoreactivity with flavopiridol treatment (Fig. 6Fg). NG2-immunostained cells present in the border zone are double immunostained for GFAP (arrows in Fig. 6Fd–f and G). Note that immunostainings for GFAP also detected NG2-negative cells (arrowheads in Fig. 6G). Thus, in agreement with prior studies,<sup>25,27,28</sup> we show here that a subset of GFAP<sup>+</sup> astrocytes concentrated at the boundary between residual spinal cord tissue and the central lesion are immunopositive for NG2 proteoglycan. In addition, we found using *in vitro* cultures that hypertrophic astrocytes induced by TGF $\beta$ 1 upregulate expression of NG2 (unpublished results). The second type of cells expressing NG2 after chronic injury were p75<sup>+</sup> Schwann cells observed inside the lesion (arrows in Fig. 6H), consistent with reports by others.<sup>27,29–31</sup> The third type of NG2<sup>+</sup> cells, observed at 4 weeks after injury in preserved white matter and gray matter, were morphologically characterized as oligodendrocyte precursor cells (OPC, stars in Fig. 6G). However, NG2<sup>+</sup>-OPC cells peak at 3 and 7 d after SCI.<sup>32–34</sup> In agreement with previous studies in references 32, 34–36, we also found that a subset of OX42<sup>+</sup> macrophages in the central lesion area are transiently immunopositive for NG2 after insult (arrows in Fig. 6I). However, large numbers of OX42<sup>+</sup> cells in the field do not express NG2 proteoglycan (arrowheads in Fig. 6I). OX42<sup>+</sup> cells have a distinct morphology, whether co-labeled with NG2 or not.<sup>34,36</sup> NG2<sup>+</sup>/fibronectin<sup>+</sup>-meninges have been observed at the section edges. However, none of NG2-expressing cells inside the spinal cord tissues appear fibronectin-positive (arrows in Fig. 6J).

Activation of microglia/macrophages peaks at 7 d after SCI during the early phase of cellular inflammation.<sup>37–39</sup> In order to evaluate the effects of systemic delayed administration of flavopiridol on SCI-induced inflammation, we examined activation of resident microglia/infiltrating macrophages using either western blot analysis or unbiased stereological assessment of Iba-1<sup>+</sup> cells. As shown in Figure 7B, flavopiridol treatment significantly reduced the SCI-induced upregulation of Iba-1 protein at 7 d post-injury. Representative immunoblots are shown in left part of

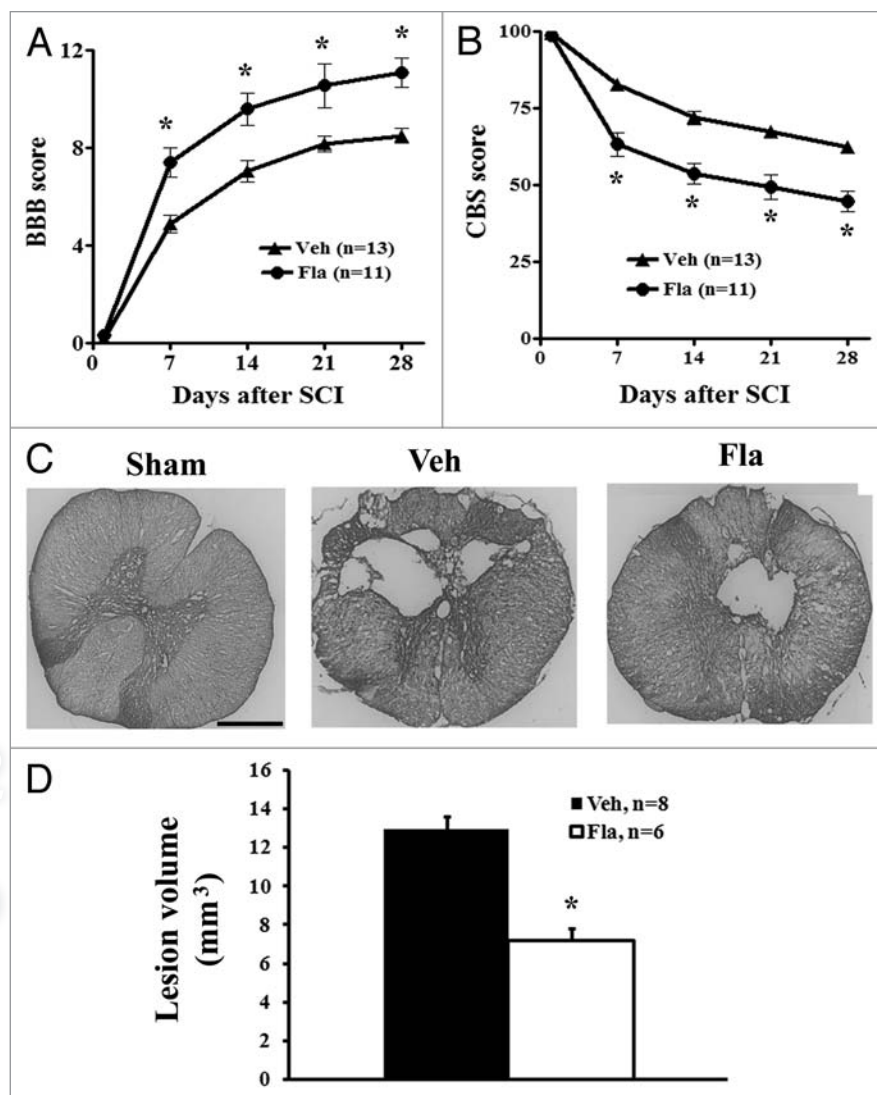


**Figure 3.** Delayed systemic treatment of flavopiridol improves functional recovery and reduces lesion volume after SCI. Both BBB (A) and CBS (B) behavioral tests showed greater functional recovery in flavopiridol treated rats. The BBB (0 = paralysis; 21 = normal), which evaluates open field locomotion, showed a difference in recovery by the first week after moderate SCI. The CBS (100 = paralysis; 0 = normal), which evaluates overall hind limb sensory-motor deficits, indicated a significant reduction in functional deficits in the flavopiridol treated group by the first week after injury. \* $p < 0.05$  vs. vehicle group.  $n = 11–13$ /group. (C) Unbiased stereological assessment of lesion volume at 28 d post-injury was performed on GFAP/DAB stained coronal sections. Representative images showed lesion cavity at 2 mm caudal to the injury center at 4 weeks after injury. Scale bars = 500  $\mu$ m. (D) Quantification analysis showed significantly reduced lesion volume in flavopiridol treated group. \* $p < 0.05$  vs. vehicle group.  $n = 6–8$ /group.

A. Flavopiridol treatment did not significantly affect the number of Iba-1<sup>+</sup> microglial/macrophages (Fig. 7C,  $p = 0.122$  vs. vehicle). Interestingly, flavopiridol treatment significantly reduced numbers of Iba-1<sup>+</sup> cells in the preserved tissue at 7 d post-injury ( $p = 0.028$  vs. vehicle) but not in the central lesion area (Fig. 7C,  $p = 0.345$  vs. vehicle), suggesting inhibition of proliferation of microglial but no significant effect on infiltration/proliferation of macrophages. Figure 7D shows lesion boundary between spared tissue and lesion cavity as indicated by GFAP staining. GFAP<sup>+</sup> astrocytes are absent in the lesion cavity after rat contusion SCI,

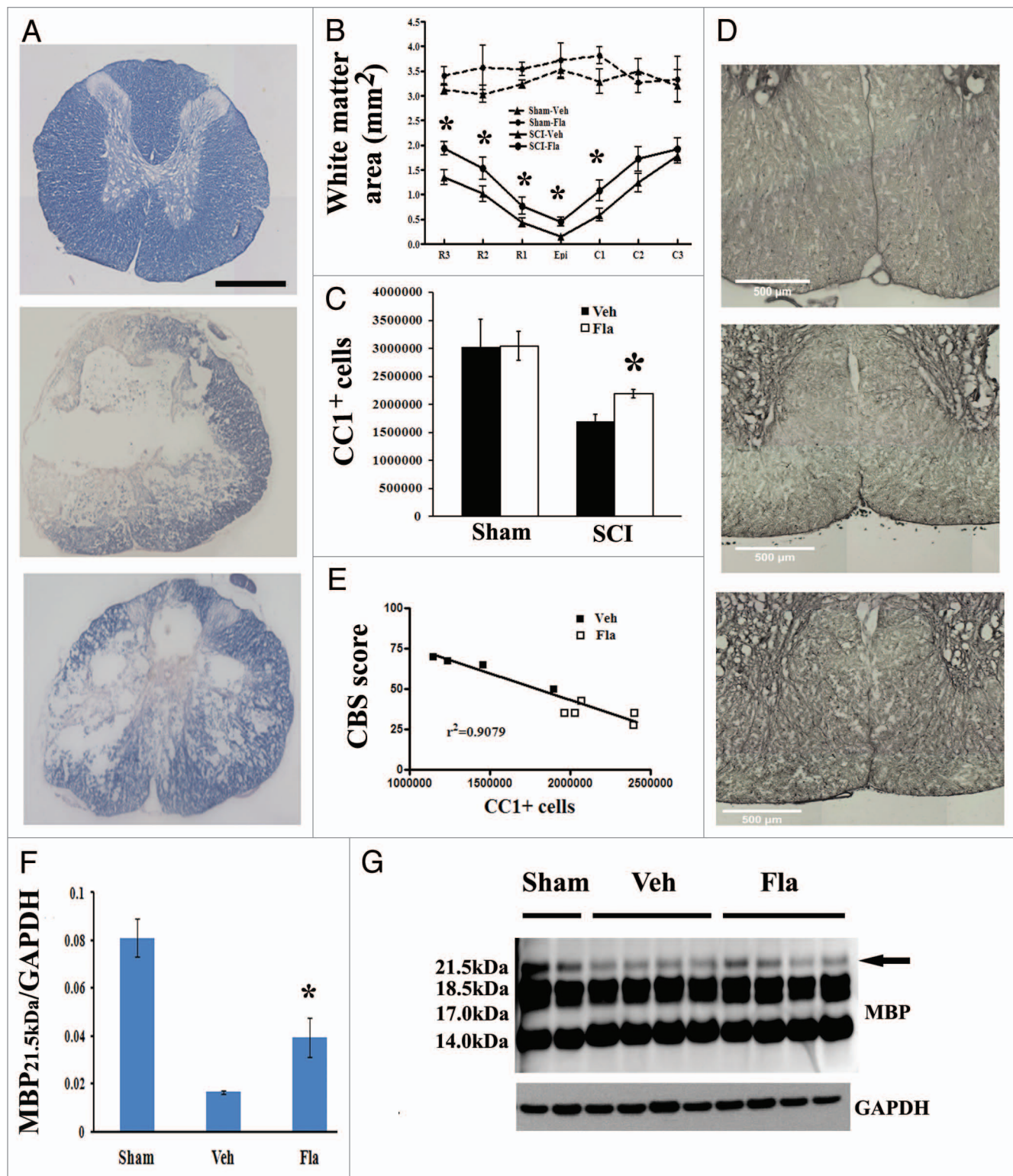


**Figure 4.** For figure legend, see page 1788.

but instead, these cells surround the lesion. Circulating macrophages infiltrate the lesion and its core, and the area with the high concentration of macrophages was labeled as lesion area, indicated in **Figure 7C and D**. The majority of Iba-1<sup>+</sup> cells in

the spared tissue are CNS resident microglia. Expression levels of Iba-1 and galectin-3 remained high at 28 d post-injury, but with significantly reduced levels in flavopiridol-treated tissue in comparison to vehicle-treated tissue (**Fig. 7E–G**).

**Figure 4 (See previous page).** Flavopiridol treatment increases number of oligodendrocytes and myelinated area in residual tissue after SCI. (A and B) Eriochrome staining for myelin was performed on spinal cord sections at 4 weeks post-injury to quantify residual white matter. Representative images at 1 mm caudal to the injury center revealed a central core lesion with spared peripheral white matter [middle part in (A)] and an increased area of spared white matter in flavopiridol treated cord [bottom part in (A)]. Quantification analysis (B) showed that flavopiridol treated subjects display significantly more remaining white matter around the lesion area than vehicle treated group at 1–3 mm rostral or 1 mm caudal to the epicenter. n = 6–8 in vehicle or flavopiridol groups, n = 3 in sham or sham + flavopiridol group. (C and D) Unbiased stereological assessment of oligodendrocytes loss at 28 d post-injury was performed on CC1/DAB stained coronal sections. Treatment with flavopiridol attenuated SCI-induced loss of CC1<sup>+</sup> mature oligodendrocytes in the preserved tissue (C). Representative images (D) of CC1/DAB staining located in both of ventromedial white matter from Sham, Vehicle- and flavopiridol-treated spinal cord. (E) Linear regression analysis comparing SCI-induced oligodendrocytes loss with CBS scores at 4 weeks post-SCI. R<sup>2</sup> = 0.9079. (F and G) Western blot analysis showed that one of the MBP isoforms (21.5 kDa) was significantly upregulated in the flavopiridol-treated group at 4 weeks post-injury. No apparent differences between the groups were found for the other MBP isomers (18.5, 17.0 and 14.0 kDa, in H). n = 4 in vehicle or flavopiridol groups, n = 2 in sham or sham + flavopiridol group. \*p < 0.05 vs. vehicle group. Scale bars = 500 μm in (A and D).

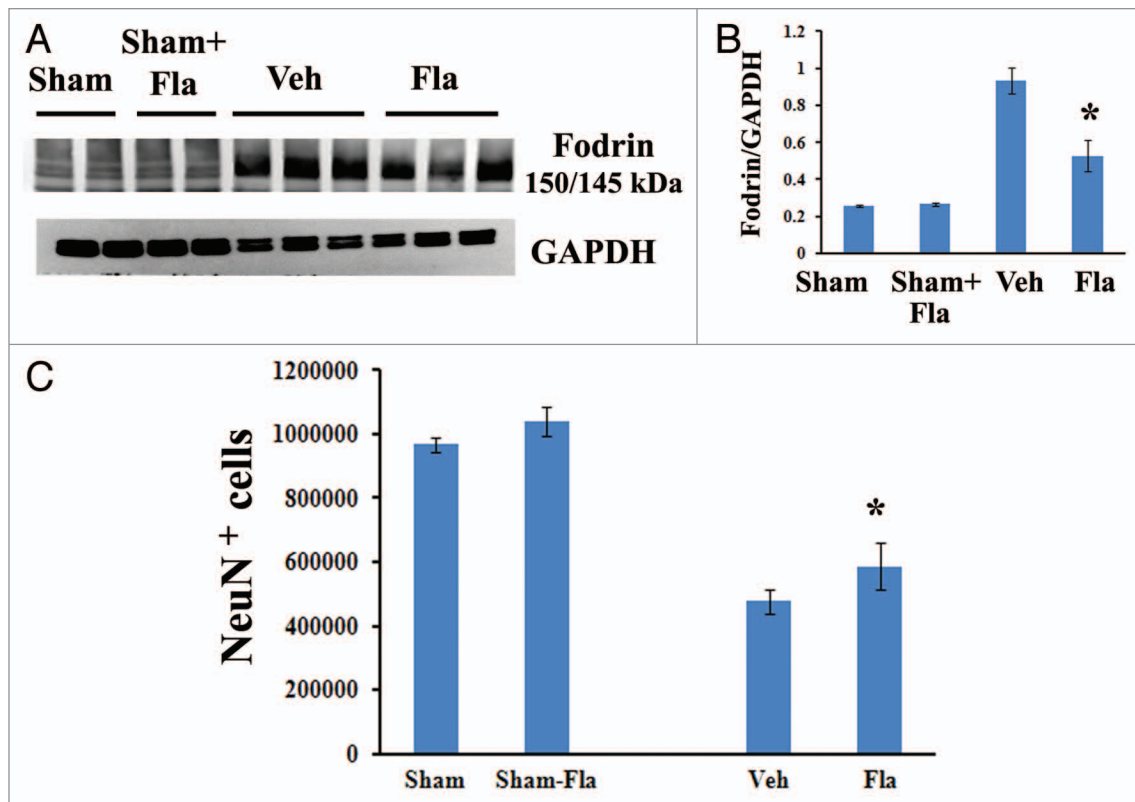


**Figure 5.** Delayed administration of flavopiridol reduces SCI-induced apoptosis and rescues neuronal cell loss. (A and B) Western blot analysis for markers of apoptosis following SCI. Flavopiridol significantly reduced the SCI-induced increases in the cleavage products of fodrin at 3 d post-injury. Representative immunoblots are shown in right part of (A). n = 3 in vehicle or flavopiridol groups, n = 2 in sham or sham + flavopiridol group. (C) Unbiased stereological assessment of neuronal loss at 28 d post-injury was performed on NeuN/DAB stained coronal sections. Treatment with flavopiridol attenuated SCI-induced loss of NeuN<sup>+</sup> neurons in the preserved gray matter (C). \*p < 0.05 vs. vehicle group. n = 6–8 in vehicle or flavopiridol groups, n = 4 in sham or sham + flavopiridol group.

To clarify the effect of systemic flavopiridol treatment on Iba-1<sup>+</sup> cells in the central lesion area, where circulating macrophages infiltrate after SCI, complete blood cell counts and differentials were performed on day 7 after flavopiridol or vehicle treatment in both injured and laminectomy-only rats. Flavopiridol administration did not affect the number of peripheral circulating white blood cells, including monocytes, lymphocytes, neutrophils, basophils and eosinophils (data not shown). Overall, these data suggest that systemic administration of flavopiridol at a dose of 1 mg/kg inhibits microglial activation without affecting the invasion of inflammatory monocytes into the lesion site.

## Discussion

Our results show that delayed systemic administration of the CDK inhibitor flavopiridol, beginning at 24 h and once daily for 7 d after injury can significantly improve motor function recovery and reduce histopathological changes after SCI. Our data also include detailed temporal measurements of cell cycle protein expression (1, 3, 7, 14 and 28 d) after SCI.

Many studies have suggested that cell cycle activation plays a pathophysiological role in CNS injury.<sup>12-17,40</sup> Cyclin D1 elevation in neurons leads to activation of CDK4/6, which then phosphorylates Rb.<sup>41</sup> Phosphorylation of Rb increases transcription

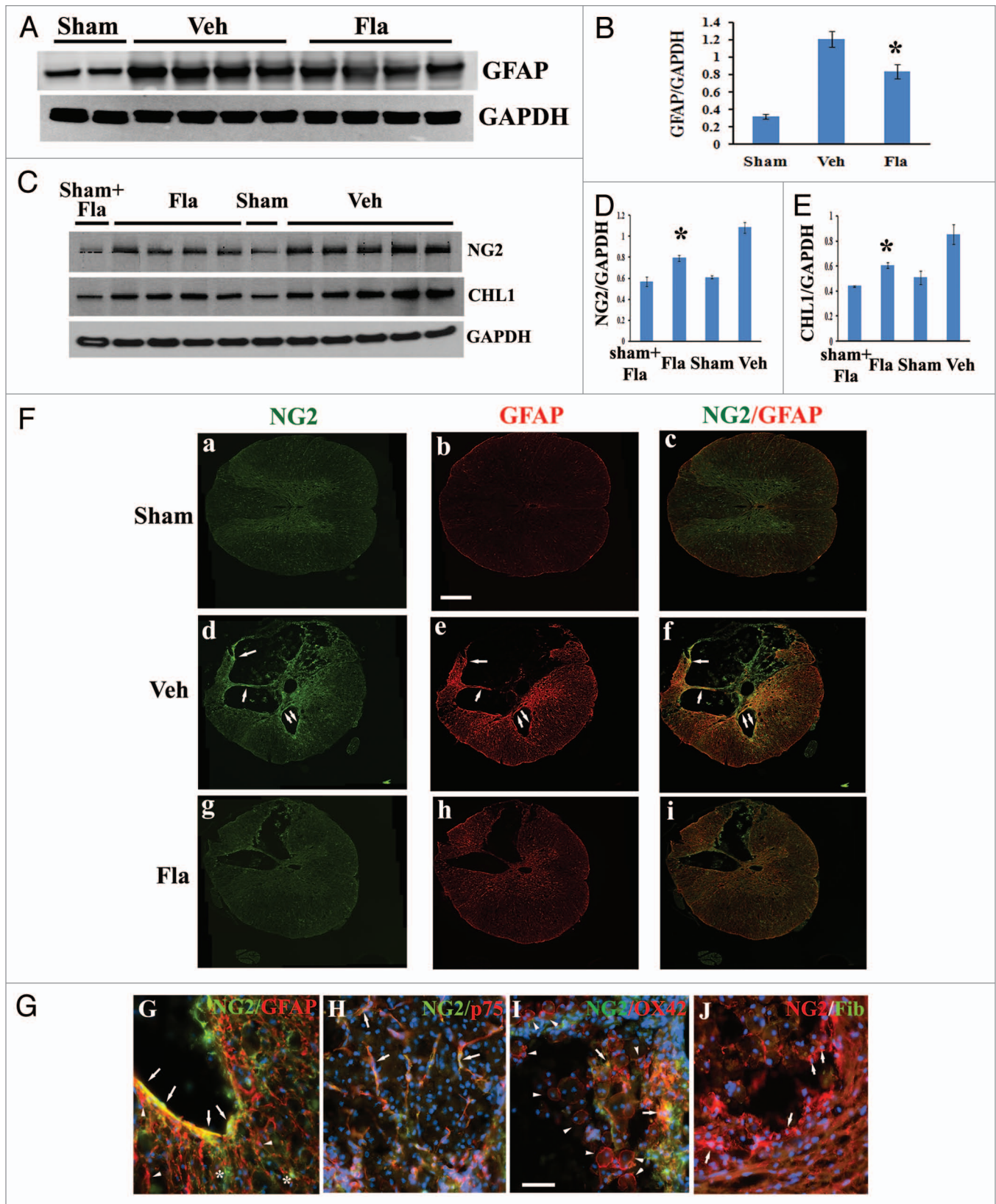


**Figure 6.** For figure legend, see page 1790.



**Figure 6 (See previous page).** Flavopiridol decreases astrocytic reactivity after SCI. (A and B) Western blot analysis showed that flavopiridol treatment significantly reduced the SCI-induced upregulation of GFAP at 4 weeks post-injury. Representative immunoblots are shown in (A). (C–E) Increases of NG2 and CHL1 expression at 4 weeks after SCI were significantly attenuated by treatment of flavopiridol. Representative immunoblots are shown in (C). \* $p < 0.05$  vs. vehicle group.  $n = 4–5$  in vehicle or flavopiridol groups,  $n = 2$  in sham or sham + flavopiridol group. (F) Wide-field high-resolution confocal images of a complete transversal section of the injured spinal cord (d–f) revealed that NG2 (green) and GFAP (red) immunoreactivity is increased throughout the cord at 4 weeks after SCI. This was attenuated by treatment with flavopiridol (g–i). Scale bars = 500  $\mu\text{m}$ . (G) NG2-immunostained cells present in the border zone were double immunostained for GFAP (arrows). Note that immunostainings for GFAP also detected NG2-negative cells (arrowheads). NG2<sup>+</sup>-oligodendrocyte precursor cells were negative for GFAP (stars). (H) NG2<sup>+</sup>/p75<sup>+</sup> Schwann cells were observed inside the lesion (arrows). (I) A subset of OX42<sup>+</sup> macrophages in the central lesion area were transiently immunopositive for NG2 after insult (arrows). However, large numbers of OX42<sup>+</sup> cells in the field did not express NG2 proteoglycan (arrowheads). (J) None of NG2-expressing cells inside the spinal cord tissues appeared fibronectin positive (arrows). Scale bars for (G–J) = 50  $\mu\text{m}$ .

of E2F pro-apoptotic targets and promotes progression of the cell to S phase of the cell cycle in both mitotic and post-mitotic cells.<sup>42,44</sup> Consistent with our previous studies in references 8 and 13, we show here that phosphorylation of Rb and expression of cyclin D1 increases at 24 h post-injury, followed by elevation of CDK4 expression at 3 d, indicating general activation of CDKs. Activation of CDK1 results in phosphorylation of numerous targets in the nucleus and mitochondria, for instance, early and robust upregulation of the E2F1 transcription factor. We also show that CDK4, as well as cyclin D1 are persistently elevated during a later phase (1–4 weeks) following injury PCNA is increased during day 3–7 post-injury, likely reflecting expression by activated microglia/macrophages. In addition, the endogenous CDK inhibitor p27, normally highly expressed in neurons and mature oligodendrocytes<sup>11,45,46</sup> is downregulated and remained at 30–40% of control during weeks 1–4.

Cyclin-dependent kinase inhibitors (CDKIs) are small peptides that block cyclin/CDKs activity, either by forming an inactive complex or by acting as a competitive ligand for CDKs. Both endogenous and exogenous CDKIs can block cell cycle progression. Flavopiridol, a semi-synthetic flavonoid derived from the bark of rohitukin,<sup>47</sup> inhibits all CDKs, reduces cyclin D1 mRNA transcription and leads to cell cycle arrest in G<sub>1</sub> or at the G<sub>2</sub>/M transition.<sup>48,49</sup> We have previously reported attenuation of Rb phosphorylation and expression of cyclin D1 by intrathecal injection of flavopiridol after SCI.<sup>13</sup> The present study confirms similar results by systemic administration. Moreover, we demonstrate that flavopiridol treatment reduces CDK4 and cyclin D1 expression chronically after SCI, further confirming the capacity of flavopiridol to inhibit cell cycle pathways in this model, and suggesting that persistent cell cycle activation after injury may reflect a positive feedback loop that can be broken with subacute cell cycle inhibitor administration. Consistent with this view, expression of the endogenous inhibitor p27 is restored toward normal levels in injured spinal cord after flavopiridol treatment.

In our prior study, flavopiridol administered centrally beginning 30 min after SCI significantly improves functional recovery.<sup>13</sup> Delayed systemic administration with a therapeutic window of 24 h post-injury in our current study represents a more clinically relevant treatment paradigm. Using the BBB scale and a battery of tests of hindlimb reflexes as well as coordinated motor activity to evaluate different motor abilities, we found significant overall improvements in flavopiridol-treated rats compared with control animals. The flavopiridol-treated group demonstrated approximately 2-point improvement in the BBB score compared

with the vehicle-treated group, reflecting the ability of rats to place their paws in plantar positions or sweep hind-limbs in walking motions. This 2-point improvement is both statistically significant and functionally meaningful.

Cavity volume assessed by GFAP staining serves as a reliable marker for CNS tissue loss in rat contusion SCI model. Flavopiridol treatment significantly reduced lesion volume. This was accompanied by a significant increase in the area of spared white matter, an effect that was associated with significantly improved hind limb function. Increased white matter sparing resulting from flavopiridol treatment was found both rostral and caudal to the lesion site, indicating higher levels of myelinated residual white matter area. Flavopiridol-treated animals had a significantly higher number of oligodendrocytes than the vehicle group, and this effect was correlated with significantly improved CBS scores ( $r^2 = 0.9079$ ). Associated with increased oligodendrocyte number was a significant upregulation of the 21.5 kDa isoform of MBP, which correlates with remyelination in multiple sclerosis.<sup>50</sup> Flavopiridol has been shown to reduce apoptosis of oligodendrocytes induced by SCI.<sup>13</sup> Thus, it is possible that the increased number of oligodendrocytes observed in the current study is due to, at least partially, attenuation of apoptosis following flavopiridol treatment.

Neuronal apoptosis is often detected in acute injured spinal cord tissue for days to months after SCI. Apoptosis evidenced by TUNEL and cleaved-caspase 3 staining increased at 3 d after SCI, with many of these apoptotic cells being neurons.<sup>13</sup> Here we show elevated levels of 150/145 kDa fodrin cleavage product at 3 d post-injury. Fodrin, also known as spectrin, is a high molecular weight (240 kDa) cytoskeletal protein that undergoes degradation catalyzed by activated proteases during apoptosis.<sup>51,52</sup> The cleavage of the 150/145 kDa fragment is both calpain-(145 kDa) and caspase-(150 kDa) mediated.<sup>53</sup> Flavopiridol treatment significantly reduced products of fodrin at 72 h after injury.

Cell cycle activation induces proliferation in mitotic cells such as astrocytes and microglia. Administration of cell cycle inhibitors—including flavopiridol, roscovitine and olomoucine— inhibits microglial and astrocyte proliferation both in vitro and in vivo.<sup>9</sup> Here we confirm similar results by quantitative western blot analysis and qualitative immunostaining. The NG2 proteoglycan, one of the core proteins of chondroitin sulfate proteoglycans (CSPGs), are the major axon growth inhibitory component of the glial scar in SCI.<sup>25,27,54,55</sup> CHL1 has been demonstrated as a glial scar component that restricts posttraumatic axonal growth.<sup>24,27</sup> Both of these molecules are highly expressed

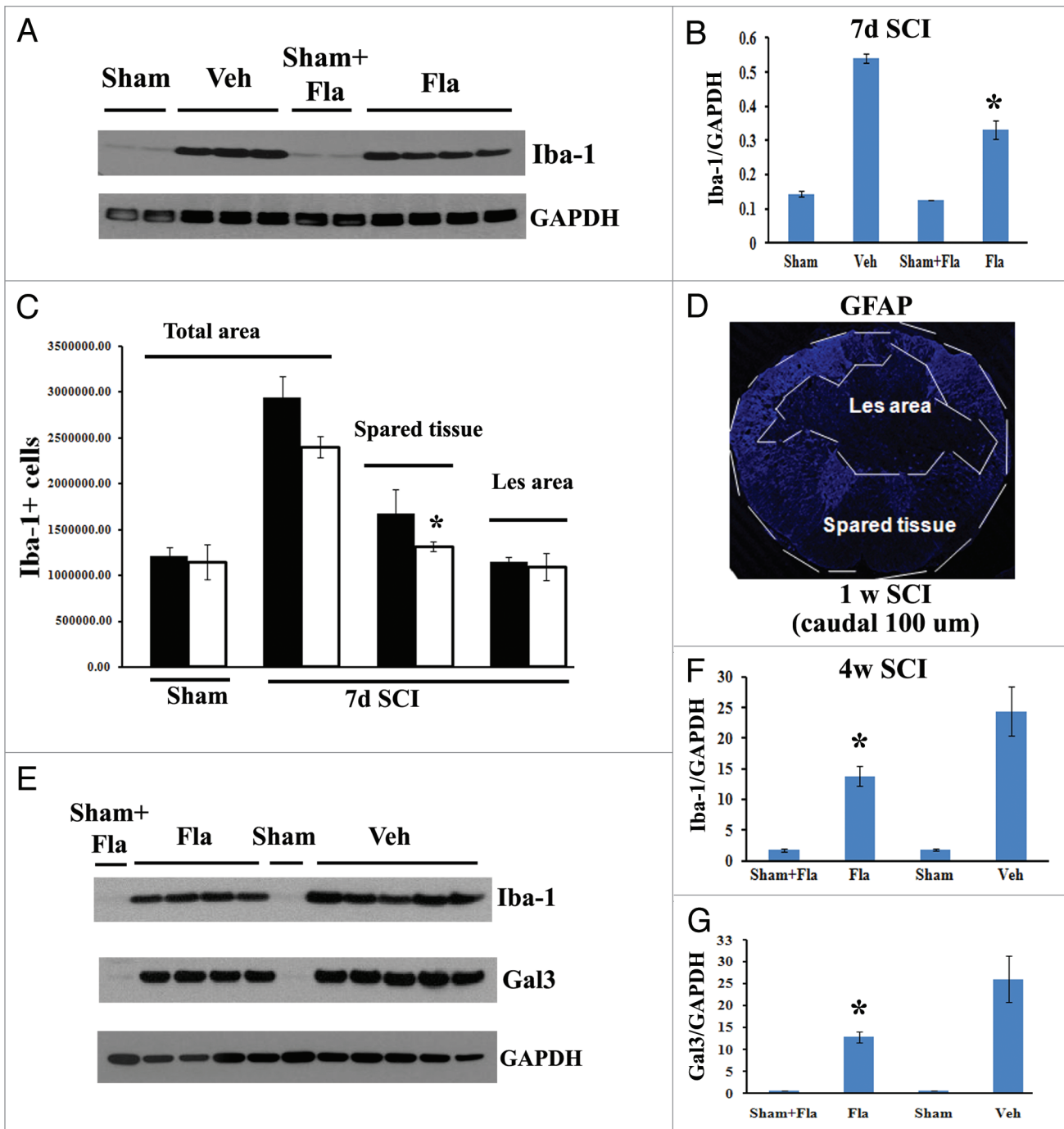


**Figure 7.** Flavopiridol inhibits the microglial/macrophage activation after SCI. (A) Western blot analysis showed that flavopiridol treatment significantly reduced the SCI-induced upregulation of Iba-1 protein at 7 d post-injury. Representative immunoblots are shown in left part of (A). (B) Treatment of flavopiridol significantly reduced numbers of Iba-1<sup>+</sup> microglia/macrophages in the preserved tissue at 7 d post-injury, but not in the central lesion area. Right image shows lesion boundary between spared tissue and lesion cavity as indicated by GFAP staining. (C) Increases of Iba-1 and galectin 3 protein expression at 4 weeks after SCI were significantly attenuated by treatment of flavopiridol. Representative immunoblots are shown in left part of (C). \*p < 0.05 vs. vehicle group. n = 3–5 in vehicle or flavopiridol groups, n = 2 in sham or sham + flavopiridol group.

by hypertrophic astrocytes after SCI. The significant reduction of NG2 and CHL1 expression observed in the present study could be the consequence of suppression of astrocytic activation by flavopiridol treatment. Thus, the ability of flavopiridol to limit scar formation may facilitate endogenous restorative potential.

Microglial activation includes both proliferation and induction of specific markers in microglia. In agreement with our previous findings in references 13 and 40, we detected significant reduction of inflammation in the SCI rats treated with flavopiridol, including decreased expression of Iba-1 and galectin 3.

We also found that flavopiridol significantly reduced numbers of Iba-1<sup>+</sup> cells in the preserved tissue at 7 d post-injury but not in the central lesion area. Combined with our results from complete blood cell count and differential assessment, these data suggest that, although systemic macrophage is not reduced by flavopiridol, microglial activation is decreased.

In conclusion, we provide evidence that cell cycle activation occurs in both early and later phases after SCI, and that systemic flavopiridol treatment administered daily for one week beginning 24 h following SCI enhances functional recovery. We attribute these effects to the ability of flavopiridol to reduce the loss of neurons and oligodendrocytes through reduction of apoptosis, to improve the local microenvironment through limitation of inflammation and to attenuate reactive astrogliosis with increased myelination.

## Materials and Methods

**Spinal cord injury and post-surgical care.** Adult male Sprague-Dawley rats weighing 275–325 g were subjected to an incomplete contusive SCI.<sup>13,56</sup> Rats were deeply anesthetized with sodium pentobarbital (65 mg/kg i.p.), while a laminectomy was performed at the level of T8 to expose a circle of dura mater. Rats were then subjected to a moderate spinal cord contusion injury by dropping a 10-g weight from a height of 2.5 cm onto an impounder positioned on the exposed dura. After SCI surgery, rats were kept on a heating pad until fully alert, and their bladders were manually expressed twice a day until a reliable bladder emptying reflex was established (10–14 d after SCI). Sham-injured rats received a laminectomy without weight drop. The experimental protocols were approved by the University of Maryland School of Medicine Animal Care and Use Committee and met all NIH guidelines. To verify injury, animals were blindly tested for hind limb motor function on day 1 after SCI. Only rats with a motor score of 1 or lower for both hind limbs (no movement or only occasional, slight movement of hind limbs) were accepted for the study.

**Drug administration.** After SCI, rats were assigned to a treatment group according to a randomized block experimental design. Flavopiridol was dissolved completely in DMSO. The concentrated solution was then diluted in sterile saline to a final concentration of 2.28% DMSO and administered intraperitoneally once daily beginning 24 h post-injury and continuing for 7 d. Rats received 1 mg/kg flavopiridol or the equivalent volume of saline with 2.28% DMSO. This regimen of flavopiridol administration was adopted due to its proven effectiveness in experimental cancer models<sup>47,57</sup> and based on our pilot studies. Complete blood cell count and differential assessment were performed by Antech diagnostics on day 7 after systemic flavopiridol or vehicle administration.

**Western blot analysis.** Rat spinal cord tissue (5 mm) centered on the injury site was obtained at 1, 3, 7, 14 and 28 d after injury, with  $n = 4$  rats per time point with an additional four laminectomy-only controls. The samples were lysed in radioimmunoprecipitation assay (RIPA) buffer (Sigma), then homogenized and sonicated.<sup>27</sup> Supernatants were collected after centrifugation at 20,600x g for 20 min at 4°C. Protein concentration was measured

by the Pierce BCA Protein Assay kit (Thermo Scientific). Equal amounts of protein were electrophoretically separated on 4 to 12% NuPAGE Novex Bis-Tris gradient gels (Invitrogen) and then transferred to nitrocellulose membranes (Invitrogen). After blocking in 5% nonfat milk for 1 h at room temperature, membranes were probed with primary antibodies (Table 1) overnight at 4°C followed by horseradish peroxidase-conjugated secondary antibodies (GE Healthcare) for 1 h at room temperature. The blots were then visualized using SuperSignal West Dura Extended Duration Substrate (Thermo Scientific), and quantified by band densitometry of scanned films using the Gel-Pro Analyzer program (Media Cybernetics, Inc.).

**Functional assessment.** Rats were assessed for hind limb function in open field locomotion on day 1 post-injury and weekly thereafter for up to 4 weeks using the Basso, Beattie and Bresnahan (BBB) open field expanded locomotor score.<sup>58</sup> Neurological functional deficits were also estimated with a combined behavioral score (CBS),<sup>22</sup> which included open field locomotion (motor score); withdrawal reflex to hind limb extension, pain and pressure; foot placing, toe spread and righting reflexes; maintenance of position on an inclined plane and swimming tests.

**Tissue processing and histopathology.** At specific times after injury, rats were anesthetized and transcardially perfused with saline followed by 4% paraformaldehyde (PFA) in PBS. Spinal cords were removed and post-fixed in 4% PFA overnight before cryoprotecting in 30% sucrose at 4°C. A 2.0-cm segment of spinal cord centered at the injury epicenter was sectioned at 20- $\mu$ m thickness and thaw-mounted onto Superfrost Plus slides (Fisher Scientific). Every twentieth section was stained with Eriochrome-cyanine RC for myelinated white matter (blue), hematoxylin for cell nuclei and eosin/phloxine (cytoplasm) to visualize cells and gray matter neuropil. The lesion epicenter was defined as the section with the least amount of spared white matter.<sup>59</sup>

**Estimation of lesion volume.** Lesion volume was assessed using the Stereologer 2000 software (Systems Planning and Analysis). Sections spaced 1 mm apart from 5 mm caudal to 5 mm rostral the injury epicenter were stained with GFAP and DAB as the chromogen for lesion volume assessment based on the Cavalieri method of unbiased stereology with a grid spacing of 200  $\mu$ m.

**Assessment of white matter sparing.** Representative slides from each set were stained with eriochrome cyanine (ECRC) and residual white matter (WM) area was calculated at the injury epicenter as well as at points rostral and caudal to the epicenter by quantifying the total area stained by ECRC.<sup>50</sup> Images were taken at 2.5x magnification and analyzed using NIH ImageJ software. The threshold level of each 8-bit image was set to display only ECRC-positive pixels, and total ECRC-positive area was calculated for each section.

**Immunohistochemistry.** Immunohistochemistry was performed on spinal cord sections at specified distances rostral and caudal to the injury epicenter.<sup>27</sup> Water-bath antigen demasking was performed in 0.01 M sodium citrate solution, pH 9.0, for 30 min at 80°C for all antigens.<sup>24</sup> Sections were fixed with 10% buffered formalin after pre-warm at room temperature and blocked for 1 h with 10% normal goat serum in PBS + 0.3% Triton

**Table 1.** Primary antibodies used

Antibody	Species	Manufacturer	Catalog no.
APC (CC1)	Mouse	Abcam	Ab 16794
CDK4	Rabbit	Santa Cruz Bio.	Sc-260
CHL1	Goat	R and D Systems	2147-CH
Cyclin D1	Rabbit	Neomarkers	RM 9104 S
E2F1	Mouse	BD PharMingen™	554213
Fibronectin	Rabbit	Abcam	ab 2413
Fodrin	Mouse	Affinity Research Products	FG 6090
Galectin 3	Mouse	Abcam	Ab 2785
GAPDH	Mouse	Stressgen	Csa 335
GFAP	Mouse	Chemicon	MAB 350
Iba-1	Rabbit	WAKO	16–20001
MBP (SMI94)	Mouse	Covance	SMI-94R
NeuN	Mouse	Chemicon	MAB 377
NG2	Rabbit	Millipore	AB 5320
NG2	Mouse	Millipore	MAB 5384
OX42	Mouse	Serotec	MCA 275R
p27	Rabbit	Santa Cruz Bio.	Sc-528
p75(NGFR)	Mouse	Chemicon	MAB 365
PCNA	Rabbit	Santa Cruz Bio.	Sc-7907
pRb ser780	Rabbit	Cell Signaling Tech.	93075

X-100. After washing, sections were incubated overnight at 4°C with primary antibodies (Table 1) and then 1 h at room temperature for fluorescent-conjugated secondary antibody (Alexa 488-conjugated goat anti-mouse, 1:400, Molecular Probes). Cell nuclei were labeled with bis-benzimide solution (Hoechst 33258 dye, 5 µg/ml in PBS, Sigma). Finally, slides were washed and mounted with an anti-fading medium. Immunofluorescence was visualized by tile scan using a Leica TCS SP5 II Tunable Spectral Confocal microscope (Leica Microsystems Inc.). The images were processed using Adobe Photoshop 7.0 software (Adobe Systems). All immunohistological staining experiments were performed with appropriate positive control tissue as well as primary/secondary-only negative controls.

**Cell counts by unbiased stereology.** *CC1*<sup>+</sup> and *NeuN*<sup>+</sup> cells. 6–8 representative subjects (based on BBB score) from the 28-d rat study were selected from each treatment group for quantification of mature oligodendrocytes (*CC1*<sup>+</sup> cells) and neurons (*NeuN*<sup>+</sup> cells) using unbiased stereology using the optical fractionators method with the aid of StereoInvestigator Software (MBF Biosciences). Sections spaced 1 mm apart from 5 mm caudal to 5 mm rostral the injury epicenter were included for counting. A sampling grid comprised of 250 µm by 250 µm squares

(150 µm by 150 µm squares in the gray matter for *NeuN*<sup>+</sup> cells) were laid over each section. Cells were counted in a 50 µm by 50 µm counting frame within each square of the counting grid with a height of 10 µm and a guard zone of 4 µm from the top of the section. *CC1*<sup>+</sup> or *NeuN*<sup>+</sup> cells were counted throughout the entire section.

***Iba-1*<sup>+</sup> cells.** StereoInvestigator Software (MBF Biosciences) was used to count the number of microglia in both the lesion and spared tissue using the optical fractionators method of unbiased stereology. Sections from the 7 d rat study spaced 1 mm apart from 5 mm caudal to 5 mm rostral the injury epicenter were stained for *Iba-1* and DAB. Contours outlining spared and lesion tissue were traced onto each section based on the GFAP staining of adjacent sections. The optical dissector had a size of 50 µm by 50 µm in the x and y axis respectively with a height of 10 µm and a guard zone of 4 µm from the top of the section. A grid spacing of 250 µm in the x axis and 250 µm in the y axis was used. Microglia were counted throughout both spared and lesion tissue.

**Sampling and statistical analysis.** All data are plotted as mean ± SEM, where “n” is the number of individual animals. Behavioral scores, lesion volume, white matter sparing and unbiased stereological analysis were performed by an investigator blinded to treatment group. All statistical analyses were conducted by using the GraphPad Prism Program, Version 3.02 for Windows (GraphPad Software). BBB and CBS scores were analyzed with two-way ANOVA and repeated measures. To determine significance between two groups, a two-tailed unpaired Student t-test was used. Statistical significance between multiple groups was conducted by one-way ANOVA with Tukey or Newman-Keuls post-hoc test. Regression analysis between behavioral scores and stereological assessment was performed by linear regression and correlation coefficient, with *r*<sup>2</sup> determined. The threshold value for significance was *p* < 0.05.

#### Disclosure of Potential Conflicts of Interest

No potential conflicts of interest were disclosed.

#### Author contributions

Conceived and designed the experiments: J.W., B.A.S., A.I.F. Performed the experiments: J.W., B.A.S., M.D., A.P.G., C.P. Analyzed the data: J.W., M.D. Wrote the paper: J.W., A.I.F. Funding the personnel: A.I.

#### Acknowledgements

Flavopiridol was provided by the NCI/Aventis. This work was supported by a National Institute of Health contract NIH-NINDS-01 (NS054221-03).

#### References

- Dumont RJ, Okonkwo DO, Verma S, Hurlbert RJ, Boulos PT, Ellegala DB, et al. Acute spinal cord injury, part I: pathophysiologic mechanisms. *Clin Neuropharmacol* 2001; 24:254-64; PMID:11586110; <http://dx.doi.org/10.1097/00002826-200109000-00002>.
- Faden AL. Experimental neurobiology of central nervous system trauma. *Crit Rev Neurobiol* 1993; 7:175-86; PMID:8221911.
- Hagg T, Oudega M. Degenerative and spontaneous regenerative processes after spinal cord injury. *J Neurotrauma* 2006; 23:264-80; PMID:16629615; <http://dx.doi.org/10.1089/neu.2006.23.263>.
- Nashmi R, Fehlings MG. Changes in axonal physiology and morphology after chronic compressive injury of the rat thoracic spinal cord. *Neuroscience* 2001; 104:235-51; PMID:11311546; [http://dx.doi.org/10.1016/S0306-4522\(01\)00009-4](http://dx.doi.org/10.1016/S0306-4522(01)00009-4).
- Sekhon LH, Fehlings MG. Epidemiology, demographics and pathophysiology of acute spinal cord injury. *Spine (Phila Pa 1976)* 2001; 26:2-12; PMID:11805601; <http://dx.doi.org/10.1097/00007632-200112151-00002>.
- Tator CH. Experimental and clinical studies of the pathophysiology and management of acute spinal cord injury. *J Spinal Cord Med* 1996; 19:206-14; PMID:9237787.

7. Tator CH. Strategies for recovery and regeneration after brain and spinal cord injury. *Inj Prev* 2002; 8:33-6; PMID:12460955; [http://dx.doi.org/10.1136/ip.8.suppl\\_4.iv33](http://dx.doi.org/10.1136/ip.8.suppl_4.iv33).
8. Di Giovanni S, Knobloch SM, Brandoli C, Aden SA, Hoffman EP, Faden AI. Gene profiling in spinal cord injury shows role of cell cycle in neuronal death. *Ann Neurol* 2003; 53:454-68; PMID:12666113; <http://dx.doi.org/10.1002/ana.10472>.
9. Wu J, Stoica BA, Faden AI. Cell cycle activation and spinal cord injury. *Neurotherapeutics* 2011; 8:221-8; PMID:21373950; <http://dx.doi.org/10.1007/s13311-011-0028-2>.
10. Greene LA, Biswas SC, Liu DX. Cell cycle molecules and vertebrate neuron death: E2F at the hub. *Cell Death Differ* 2004; 11:49-60; PMID:14647236; <http://dx.doi.org/10.1038/sj.cdd.4401341>.
11. Nguyen MD, Boudreau M, Kriz J, Couillard-Després S, Kaplan DR, Julien JP. Cell cycle regulators in the neuronal death pathway of amyotrophic lateral sclerosis caused by mutant superoxide dismutase 1. *J Neurosci* 2003; 23:2131-40; PMID:12657672.
12. Tian DS, Yu ZY, Xie MJ, Bu BT, Witte OW, Wang W. Suppression of astroglial scar formation and enhanced axonal regeneration associated with functional recovery in a spinal cord injury rat model by the cell cycle inhibitor olomoucine. *J Neurosci Res* 2006; 84:1053-63; PMID:16862564; <http://dx.doi.org/10.1002/jnr.20999>.
13. Byrnes KR, Stoica BA, Fricke S, Di Giovanni S, Faden AI. Cell cycle activation contributes to post-mitotic cell death and secondary damage after spinal cord injury. *Brain* 2007; 130:2977-92; PMID:17690131; <http://dx.doi.org/10.1093/brain/awm179>.
14. Tian DS, Xie MJ, Yu ZY, Zhang Q, Wang YH, Chen B, et al. Cell cycle inhibition attenuates microglia induced inflammatory response and alleviates neuronal cell death after spinal cord injury in rats. *Brain Res* 2007; 1135:177-85; PMID:17188663; <http://dx.doi.org/10.1016/j.brainres.2006.11.085>.
15. Di Giovanni S, Movsesyan V, Ahmed F, Cernak I, Schinelli S, Stoica B, et al. Cell cycle inhibition provides neuroprotection and reduces glial proliferation and scar formation after traumatic brain injury. *Proc Natl Acad Sci USA* 2005; 102:8333-8; PMID:15923260; <http://dx.doi.org/10.1073/pnas.0500989102>.
16. Hilton GD, Stoica BA, Byrnes KR, Faden AI. Roscovitine reduces neuronal loss, glial activation and neurologic deficits after brain trauma. *J Cereb Blood Flow Metab* 2008; 28:1845-59; PMID:18612315; <http://dx.doi.org/10.1038/jcbfm.2008.75>.
17. Kabadi SV, Stoica BA, Byrnes KA, Hanscom M, Loane DJ, Faden AI. Selective CDK inhibitor limits neuroinflammation and progressive neurodegeneration after brain trauma. [Epub ahead of print]. *J Cereb Blood Flow Metab* 2012; 32:137-49. PMID:21829212; <http://dx.doi.org/10.1038/jcbfm.2011.117>.
18. Zhu Z, Zhang Q, Yu Z, Zhang L, Tian D, Zhu S, et al. Inhibiting cell cycle progression reduces reactive astrogliosis initiated by scratch injury in vitro and by cerebral ischemia in vivo. *Glia* 2007; 55:546-58; PMID:17243097; <http://dx.doi.org/10.1002/glia.20476>.
19. Wang W, Redecker C, Yu ZY, Xie MJ, Tian DS, Zhang L, et al. Rat focal cerebral ischemia induced astrocyte proliferation and delayed neuronal death are attenuated by cyclin-dependent kinase inhibition. *J Clin Neurosci* 2008; 15:278-85; PMID:18207409; <http://dx.doi.org/10.1016/j.jocn.2007.02.004>.
20. Malumbres M, Barbacid M. Cell cycle, CDKs and cancer: a changing paradigm. *Nat Rev Cancer* 2009; 9:153-66; PMID:19238148; <http://dx.doi.org/10.1038/nrc2602>.
21. Bracklen MB, Holford TR. Effects of timing of methylprednisolone or naloxone administration on recovery of segmental and long-tract neurological function in NASCIS 2. *J Neurosurg* 1993; 79:500-7; PMID:8410217; <http://dx.doi.org/10.3171/jns.1993.79.4.0500>.
22. Gale K, Kerasidis H, Wrathall JR. Spinal cord contusion in the rat: behavioral analysis of functional neurologic impairment. *Exp Neurol* 1985; 88:123-34; PMID:3979506; [http://dx.doi.org/10.1016/0014-4886\(85\)90118-9](http://dx.doi.org/10.1016/0014-4886(85)90118-9).
23. Silver J, Miller JH. Regeneration beyond the glial scar. *Nat Rev Neurosci* 2004; 5:146-56; PMID:14735117; <http://dx.doi.org/10.1038/nrn1326>.
24. Jakovcevski I, Wu J, Karl N, Leshchynska I, Sytnyk V, Chen J, et al. Glial scar expression of CHL1, the close homolog of the adhesion molecule L1, limits recovery after spinal cord injury. *J Neurosci* 2007; 27:7222-33; PMID:17611275; <http://dx.doi.org/10.1523/JNEUROSCI.0739-07.2007>.
25. Alonso G. NG2 proteoglycan-expressing cells of the adult rat brain: possible involvement in the formation of glial scar astrocytes following stab wound. *Glia* 2005; 49:318-38; PMID:15494983; <http://dx.doi.org/10.1002/glia.20121>.
26. Tan AM, Zhang W, Levine JM. NG2: a component of the glial scar that inhibits axon growth. *J Anat* 2005; 207:717-25; PMID:16367799; <http://dx.doi.org/10.1111/j.1469-7580.2005.00452.x>.
27. Wu J, Leung PY, Sharp A, Lee HJ, Wrathall JR. Increased expression of the close homolog of the adhesion molecule L1 in different cell types over time after rat spinal cord contusion. *J Neurosci Res* 2011; 89:628-38; PMID:21337374; <http://dx.doi.org/10.1002/jnr.22598>.
28. Wu D, Shibuya S, Miyamoto O, Itano T, Yamamoto T. Increase of NG2-positive cells associated with radial glia following traumatic spinal cord injury in adult rats. *J Neurocytol* 2005; 34:459-69; PMID:16902766; <http://dx.doi.org/10.1007/s11068-006-8998-4>.
29. Stegmüller J, Schneider S, Hellwig A, Garwood J, Trotter J. AN2, the mouse homologue of NG2, is a surface antigen on glial precursor cells implicated in control of cell migration. *J Neurocytol* 2002; 31:497-505; PMID:14501219; <http://dx.doi.org/10.1023/A:1025743731306>.
30. Jones LL, Sajed D, Tuszynski MH. Axonal regeneration through regions of chondroitin sulfate proteoglycan deposition after spinal cord injury: a balance of permissiveness and inhibition. *J Neurosci* 2003; 23:9276-88; PMID:14561854.
31. McTigue DM, Tripathi R, Wei P. NG2 colocalizes with axons and is expressed by a mixed cell population in spinal cord lesions. *J Neuropathol Exp Neurol* 2006; 65:406-20; PMID:16691121; <http://dx.doi.org/10.1097/01.jnen.0000218447.32320.52>.
32. Zai LJ, Wrathall JR. Cell proliferation and replacement following contusive spinal cord injury. *Glia* 2005; 50:247-57; PMID:15739189; <http://dx.doi.org/10.1002/glia.20176>.
33. Lytle JM, Chittajallu R, Wrathall JR, Gallo V. NG2 cell response in the CNP-EGFP mouse after contusive spinal cord injury. *Glia* 2009; 57:270-85; PMID:18756526; <http://dx.doi.org/10.1002/glia.20755>.
34. Wu J, Yoo S, Wilcock D, Lytle JM, Leung PY, Colton CA, et al. Interaction of NG2(+) glial progenitors and microglia/macrophages from the injured spinal cord. *Glia* 2010; 58:410-22; PMID:19780197.
35. Butt AM, Kiff J, Hubbard P, Berry M. Synantocytes: new functions for novel NG2 expressing glia. *J Neurocytol* 2002; 31:551-65; PMID:14501223; <http://dx.doi.org/10.1023/A:1025751900356>.
36. Lytle JM, Vicini S, Wrathall JR. Phenotypic changes in NG2(+) cells after spinal cord injury. *J Neurotrauma* 2006; 23:1726-38; PMID:17184184; <http://dx.doi.org/10.1089/neu.2006.23.1726>.
37. Popovich PG, Wei P, Stokes BT. Cellular inflammatory response after spinal cord injury in Sprague-Dawley and Lewis rats. *J Comp Neurol* 1997; 377:443-64; PMID:8989657; [http://dx.doi.org/10.1002/\(SICI\)1096-9861\(19970120\)377:3<443::AID-CNE10>3.0.CO;2-S](http://dx.doi.org/10.1002/(SICI)1096-9861(19970120)377:3<443::AID-CNE10>3.0.CO;2-S).
38. Carlson SL, Parrish ME, Springer JE, Doty K, Dossett L. Acute inflammatory response in spinal cord following impact injury. *Exp Neurol* 1998; 151:77-88; PMID:9582256; <http://dx.doi.org/10.1006/exnr.1998.6785>.
39. Beck KD, Nguyen HX, Galvan MD, Salazar DL, Woodruff TM, Anderson AJ. Quantitative analysis of cellular inflammation after traumatic spinal cord injury: evidence for a multiphasic inflammatory response in the acute to chronic environment. *Brain* 2010; 133:433-47; PMID:20085927; <http://dx.doi.org/10.1093/brain/awp322>.
40. Cernak I, Stoica B, Byrnes KR, Di Giovanni S, Faden AI. Role of the cell cycle in the pathobiology of central nervous system trauma. *Cell Cycle* 2005; 4:1286-93; PMID:16082214; <http://dx.doi.org/10.4161/cc.4.9.1996>.
41. Herwig S, Strauss M. The retinoblastoma protein: a master regulator of cell cycle, differentiation and apoptosis. *Eur J Biochem* 1997; 246:581-601; PMID:9219514; <http://dx.doi.org/10.1111/j.1432-0339.1997.t01-2-00581.x>.
42. Kitagawa M, Higashi H, Jung HK, Suzuki-Takahashi I, Ikeda M, Tamai K, et al. The consensus motif for phosphorylation by cyclin D1-Cdk4 is different from that for phosphorylation by cyclin A/E-Cdk2. *EMBO J* 1996; 15:7060-9; PMID:9003781.
43. Park DS, Morris EJ, Bremner R, Keramaris E, Padmanabhan J, Rosenbaum M, et al. Involvement of retinoblastoma family members and E2F/DP complexes in the death of neurons evoked by DNA damage. *J Neurosci* 2000; 20:3104-14; PMID:10777774.
44. Sears RC, Nevins JR. Signaling networks that link cell proliferation and cell fate. *J Biol Chem* 2002; 277:11617-20; PMID:11805123; <http://dx.doi.org/10.1074/jbc.R100063200>.
45. Durand B, Gao FB, Raff M. Accumulation of the cyclin-dependent kinase inhibitor p27/Kip1 and the timing of oligodendrocyte differentiation. *EMBO J* 1997; 16:306-17; PMID:9029151; <http://dx.doi.org/10.1093/emboj/16.2.306>.
46. Tokumoto YM, Apperly JA, Gao FB, Raff MC. Posttranscriptional regulation of p18 and p27 Cdk inhibitor proteins and the timing of oligodendrocyte differentiation. *Dev Biol* 2002; 245:224-34; PMID:11969268; <http://dx.doi.org/10.1006/dbio.2002.0626>.
47. Newcomb EW, Tamasdan C, Entzminger Y, Arena E, Schnee T, Kim M, et al. Flavopiridol inhibits the growth of GL261 gliomas in vivo: implications for malignant glioma therapy. *Cell Cycle* 2004; 3:230-4; PMID:14712094; <http://dx.doi.org/10.4161/cc.3.2.667>.
48. Dai Y, Grant S. Small molecule inhibitors targeting cyclin-dependent kinases as anticancer agents. *Curr Oncol Rep* 2004; 6:123-30; PMID:14751090; <http://dx.doi.org/10.1007/s11912-004-0024-3>.
49. Swanton C. Cell cycle targeted therapies. *Lancet Oncol* 2004; 5:27-36; PMID:14700606; [http://dx.doi.org/10.1016/S1470-2045\(03\)01321-4](http://dx.doi.org/10.1016/S1470-2045(03)01321-4).
50. Capello E, Voskuhl RR, McFarland HF, Raine CS. Multiple sclerosis: re-expression of a developmental gene in chronic lesions correlates with remyelination. *Ann Neurol* 1997; 41:797-805; PMID:9189041; <http://dx.doi.org/10.1002/ana.410410616>.
51. Siman R, Baudry M, Lynch G. Brain fodrin: substrate for calpain I, an endogenous calcium-activated protease. *Proc Natl Acad Sci USA* 1984; 81:3572-6; PMID:6328521; <http://dx.doi.org/10.1073/pnas.81.11.3572>.
52. Siman R, McIntosh TK, Soltesz KM, Chen Z, Neumar RW, Roberts VL. Proteins released from degenerating neurons are surrogate markers for acute brain damage. *Neurobiol Dis* 2004; 16:311-20; PMID:15193288; <http://dx.doi.org/10.1016/j.nbd.2004.03.016>.

53. Saatman KE, Creed J, Raghupathi R. Calpain as a therapeutic target in traumatic brain injury. *Neurotherapeutics* 2010; 7:31-42; PMID:20129495; <http://dx.doi.org/10.1016/j.nurt.2009.11.002>.
54. Morgenstern DA, Asher RA, Fawcett JW. Chondroitin sulphate proteoglycans in the CNS injury response. *Prog Brain Res* 2002; 137:313-32; PMID:12440375; [http://dx.doi.org/10.1016/S0079-6123\(02\)37024-9](http://dx.doi.org/10.1016/S0079-6123(02)37024-9).
55. Trotter J, Karram K, Nishiyama A. NG2 cells: Properties, progeny and origin. *Brain Res Rev* 2010; 63:72-82; PMID:20043946; <http://dx.doi.org/10.1016/j.brainresrev.2009.12.006>.
56. Yakovlev AG, Faden AI. Sequential expression of *c-fos* protooncogene, TNF $\alpha$  and dynorphin genes in spinal cord following experimental traumatic injury. *Mol Chem Neuropathol* 1994; 23:179-90; PMID:7702707; <http://dx.doi.org/10.1007/BF02815410>.
57. Mason KA, Hunter NR, Raju U, Ariga H, Husain A, Valdecanas D, et al. Flavopiridol increases therapeutic ratio of radiotherapy by preferentially enhancing tumor radioresponse. *Int J Radiat Oncol Biol Phys* 2004; 59:1181-9; PMID:15234054; <http://dx.doi.org/10.1016/j.ijrobp.2004.03.003>.
58. Basso DM, Beattie MS, Bresnahan JC. A sensitive and reliable locomotor rating scale for open field testing in rats. *J Neurotrauma* 1995; 12:1-21; PMID:7783230; <http://dx.doi.org/10.1089/neu.1995.12.1>.
59. Grossman SD, Rosenberg LJ, Wrathall JR. Temporal-spatial pattern of acute neuronal and glial loss after spinal cord contusion. *Exp Neurol* 2001; 168:273-82; PMID:11259115; <http://dx.doi.org/10.1006/exnr.2001.7628>.

© 2012 Landes Bioscience.  
Do not distribute.